Modeling of Cognitive Mobile Molecular Communication in a Biological Microfluidic Cylindrical Channel

Shivam Thakker*, Dhaval K. Patel†, *Member, IEEE*, Kirtan Kalaria‡, *Student Member, IEEE*,
Miguel López-Benítez§, *Senior Member, IEEE*, Janne J. Lehtomäki¶, *Member, IEEE*
*Khoury College of Computer Science, Northeastern University, Boston 02115, MA, US
†‡School of Engineering and Applied Science, Ahmedabad University, Ahmedabad 380009, India
§Department of Electrical Engineering and Electronics, University of Liverpool, L69 3GJ Liverpool, U.K.
§ARIES Research Centre, Antonio de Nebrija University, 28248 Madrid, Spain
¶ Centre for Wireless Communications, University of Oulu, 90014 Oulu, FI
Email:*†‡{shivam.t1, dhaval.patel, kirtan.k}@ahduni.edu.in,
§M.Lopez-Benitez@liverpool.ac.uk,¶janne.lehtomaki@oulu.fi

***Abstract*—In the field of targeted drug delivery and pathogenesis monitoring, a Diffusive Molecular Communication (DMC) channel is considered a promising channel model. While the current DMC state-of-the-art literature provides in-depth analysis for channel modeling across various molecular communication systems, it does not include the realistic scenarios of mobile molecular communication, which are crucial for targeted drug delivery systems. In this work, a micro-cylindrical channel for a DMC system similar to a human blood vessel is modeled, considering the coexistence of a primary and a secondary link in a mobile molecular communication scenario. Further, the priority of the primary link is considered to be higher than that of the secondary link. The proposed model overcomes the limitations of previous work by formulating the Concentration Green's Function (CGF) for biological cylindrical channels. It considers the mobility of the receiver and asymmetry in the radial, axial, and azimuthal directions. Furthermore, the effect of various channel parameters such as anomalous diffusion, degradation rate, and channel radius on the concentration observed at the receiver is also shown.**

***Index Terms*—Mobile Molecular Communication, Cognitive Communication, Cylindrical environment, Concentration Green Function (CGF), Targeted drug delivery**

I. INTRODUCTION

Molecular Communication (MC) has emerged as a cutting-edge research field at the nano-scale with numerous applications in healthcare. MC has revolutionized nano-scale communication by encoding information into molecules that diffuse through the channel, collide with surrounding objects, and are decoded by the receiver, creating an MC link between the transmitter and receiver. Researchers are making significant strides in enhancing the reliability and efficiency of MC systems by using multiple types of molecules, creating more accurate and sensitive receivers, and designing novel techniques for the modulation and demodulation of molecular signals.

Many molecular communication models and scenarios are currently being studied to improve communication at the molecular level. Extensive research has been carried out that considers unbounded environment [1] [2]. However, this assumption is not relevant to realistic scenarios. Recent research [3] has also considered a bounded spherical environment, which incorporated a DMC system considering a single point transmitter and a receiver consisting of ligand receptors. However, the assumption that the environment is spherical is also not suited to real-life biological scenarios due to symmetry. Further, [4] also considers an MC system in a confined microfluidic channel and compares the achievable rates for different propagation schemes. However, a more realistic assumption would be to consider a cylindrical channel that resembles the blood vessels in the human body. Authors in [5] considered a point-to-point DMC system in a biological cylindrical environment and derived an expression of CGF of diffusion considering the asymmetry in radial, axial, and azimuthal directions and verified it using Particle-Based Simulation (PBS).

In [6], the different molecules encoded information within a static MC system, and the achievable rate was derived considering free diffusion environments. Later, it was realized that considering the static scenario is not very apt. Hence, Felicetti et al. [7] proposed a decoding scheme considering mobile transmitter and static receiver. A study [8] proposed a framework for a mobile ad-hoc molecular network. It comprises mobile nanomachines that collect information on the concentration of molecules from their surroundings and send it to a mobile central unit. The central unit then takes actions based on the messages received. The authors in [9] considered a 3D unbounded environment with a mobile transmitter and receiver and proposed an efficient communication method taking into account multiple measurements to increase the accuracy of messages detected at the receiving end.

Recent advances in early disease detection and targeted drug delivery [10] have led to scenarios where multiple MC links could communicate simultaneously [11]. In [12], the author considered the coexistence of multiple links commu-

nicating simultaneously in a bounded cylindrical environment. They derived the CGF considering anomalous diffusion, which was validated using PBS.

A. Motivation

The work is motivated by the need for more research conducted with more realistic assumptions. Artificial nanobots injected in the blood vessel for targeted drug delivery would be mobile inside the channel. Hence, cylindrical channel and mobile molecular communication assumptions are deemed more practical for targeted drug delivery. To the best of our knowledge, no previous study has considered mobile molecular communication in a cylindrical channel while considering cognitive communication. Studying cognitive communication is also significant, as multiple artificial links deployed by humans could function simultaneously in co-existence with natural biological links. For instance, there could be multiple artificial links or an artificial link that communicates in parallel with the natural MC link, which holds a higher priority. Hence, the interference at the high-priority link should be minimal. For instance, a link carrying information on cancer cells should be prioritized over a link carrying information on body temperature or blood sugar levels. Therefore, mathematical modeling of such a scenario is necessary to maintain a particular Quality of Service (QOS) at the natural link.

B. Contributions

The major contributions of this work are as follows :

- A mathematical framework for cognitive molecular communication in a cylindrical channel considering mobile molecular communication and anomalous diffusion is proposed, and a CGF is derived.
- The effect of various channel parameters such as channel radius and degradation rate on the channel response is shown.
- An expression for the maximum number of molecules the secondary transmitter could transmit to control the interference at the primary link is derived.

The remainder of this paper is organized as follows. Section II presents the system model and anomalous diffusion considered in this work. Section III details the derivation of the CGF for biological cylindrical and mobile molecular communication channels. Numerical results are discussed in Section IV. Finally, the conclusion and future work are discussed in Section V.

II. SYSTEM MODEL

A. Network Model

Fig. 1 depicts the MC system adopted in this work. It consists of a static point transmitter and a mobile spherical receiver inside a cylindrical environment. The collision among the particles inside the channel is ignored and the molecules follow the Fick's second law of diffusion to flow inside the channel [13], given as

$$\frac{\partial c(t)}{\partial t} = D\Delta^2 c(t) \tag{1}$$

where D is the diffusion coefficient, Δ^2 is the Laplacian operator and $c(t)$ is the concentration of the molecules received at time t. A cylindrical coordinate system is used to denote any point in the cylindrical environment and is described using (ρ, ϕ, z) which represent the radial, axial, and azimuthal coordinates, respectively. This environment is constrained by

$$0 \leq \rho \leq \rho_{ch},\ 0 \leq \phi < 2\pi,\ z \geq 0 \tag{2}$$

where, ρ_{ch} is the channel radius. It is assumed that every information molecule will undergo a degradation reaction while traveling in the cylinder and can transform into another molecule that cannot bind with the receptor.

As multiple links are considered, the primary transmitter (TX_p) located at $(\rho_{TX_p}, \phi_{TX_p}, z_{TX_p})$ communicates with the spherical primary receiver (RX_p) with radius r_p and center $(\rho_{RX_p}, \phi_{RX_p}, z_{RX_p})$ in the presence of another link where a secondary transmitter (TX_s) located at $(\rho_{TX_s}, \phi_{TX_s}, z_{TX_s})$ communicates with the spherical receiver (RX_s) with radius r_s and center $(\rho_{RX_s}, \phi_{RX_s}, z_{RX_s})$. Here, the transmitter is considered to be static, and the receivers are considered to be freely mobile in the cylindrical channel, as illustrated in Fig. 2. The receiver exhibits two modes of motion: the run mode and the tumble mode. In run mode, the receiver moves only axially along the cylinder without changing its direction, whereas, in tumble mode, the receiver changes its direction with time. The receiver's direction of motion is described by its angle of motion $\theta_{rad}(.)$ in the radial plane and and angle of motion $\theta_z(.)$ from the axis in the axial plane. The change in the two angles due to diffusion in every Δt time is given by

$$\theta_{rad}(t + \Delta t) = \theta_{rad}(t) \pm \sqrt{2D_r \Delta t} \tag{3}$$

$$\theta_{ax}(t + \Delta t) = \theta_{ax}(t) \pm \sqrt{2D_r \Delta t} \tag{4}$$

where D_r is the rotational diffusion coefficient assuming omnidirectionally uniform diffusion. As a bounded channel is considered, the receiver can collide with the cylindrical wall.

B. Anomalous Diffusion

Anomalous diffusion is a diffusion process that has a relationship between the Mean Squared Displacement (MSD) of the molecules and time. It can be mathematically represented using fractional diffusion equation [14] as

$$D(t) = \alpha D t^{\alpha - 1} \tag{5}$$

where α is the diffusion exponent, which is responsible for the type of diffusion and it ranges between $[0, 2]$. For $\alpha < 1$ it is said to be in the sub-diffusion region, for $\alpha = 1$ it is normal diffusion, and for $\alpha > 1$ it is in the super-diffusion region. Fig. 3 shows the change in the diffusion coefficient with respect to time.

III. CONCENTRATION GREEN'S FUNCTION IN A BIOLOGICAL CYLINDRICAL CHANNEL CONSIDERING MOBILE MOLECULAR COMMUNICATION

In this section, the expression for the CGF is derived for the cylindrical channel considering mobile molecular communication. Let the concentration of molecules at any time t and position $(\rho(t), \phi(t), z(t))$ for the given initial time instant t_0 and TX position $(\rho_{tx}, \phi_{tx}, z_{tx})$ be

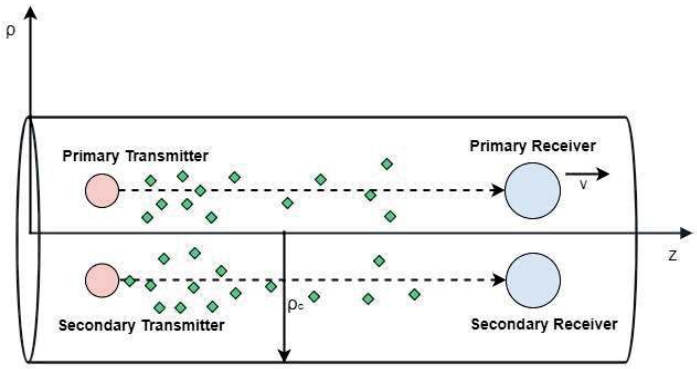

Fig. 1: Cylindrical channel exhibiting multiple MC links while considering a mobile receiver.

$C(\rho(t), \phi(t), z(t), t; \rho_{tx}, \phi_{tx}, z_{tx}, t_0)$. It can be written as $C(t; t_0)$ for simplicity of notation. Note that here, the position of the point $(\rho(t), \phi(t), z(t))$ changes at every Δt time increment as follows.

$$\rho(t + \Delta t) = \rho(t) + v_r \Delta t \sin(\theta_{ax}(t)) \tag{6}$$
$$\phi(t + \Delta t) = \phi(t) + \theta_{rad}(t) \tag{7}$$
$$z(t + \Delta t) = z(t) + v_r \Delta t \cos(\theta_{ax}(t)) \tag{8}$$

where, v_r is the velocity of the receiver. The rate of change of concentration is given by the Fick's diffusion-advection equation as

$$\frac{\partial C(t;t_0)}{\partial t} = D(t - t_0)\Delta^2 C(t;t_0) - (v\hat{u}) \cdot (\Delta C(t;t_0)) + I(t;t_0) - kC(t;t_0) \tag{9}$$

where, D is the diffusion coefficient, Δ^2 is the Laplacian operator, Δ is the gradient operator, k is the degradation constant, $\hat{u}$ is the unit vector along axial direction, and $I(t;t_0)$ is the impulsive point source at $t = t_0$ given by $I(t;t_0) = \frac{\delta(\rho(t)-\rho_{tx})}{\rho(t)}\ \delta(\phi(t) - \phi_{tx})\ \delta(z(t) - z_{tx})\ \delta(t - t_0)$. Simplifying

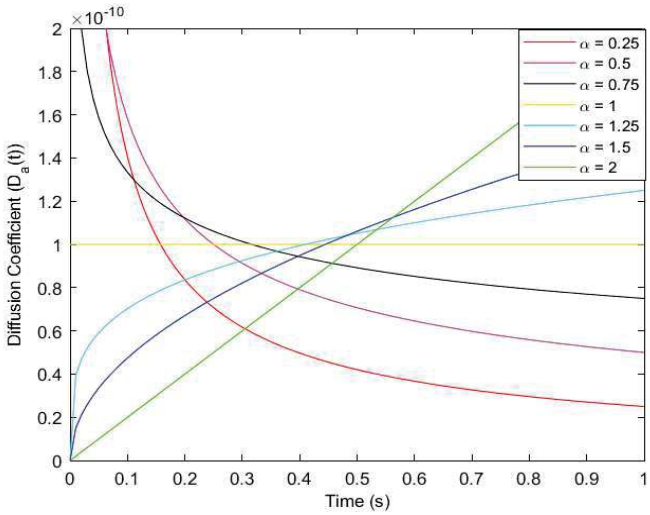

Fig. 3: Anomalous diffusion under values of different diffusion exponent.

(9) as per the Fick's equation for cylindrical coordinates,

$$\begin{aligned}\frac{\partial C(t;t_0)}{\partial t} =& D(t - t_0)\frac{\partial^2 C(t;t_0)}{\partial \rho^2(t)} + \frac{D(t - t_0)}{\rho(t)}\frac{\partial C(t;t_0)}{\partial \rho(t)} \\ &+ \frac{D(t - to)}{\rho^2(t)}\frac{\partial^2 C(t;t_0)}{\partial \phi^2(t)} + D(t - t_0)\frac{\partial^2 C(t;t_0)}{\partial z^2(t)} \\ &- v\frac{\partial C(t;t_0)}{\partial z(t)} - kC(t;t_0) + \frac{\delta(\rho(t) - \rho_{tx})}{\rho(t)}\delta(\phi(t) \\ &- \phi_{tx})\delta(z(t) - z_{tx})\delta(t - t_0)\end{aligned} \tag{10}$$

The concentration term can be obtained by multiplying the radial-azimuthal term with the axial term.

$$C(t;t_0) = C_{\rho\phi}(t;t_0) \times C_z(t;t_0) \tag{11}$$

Now, applying the third type robin boundary condition of

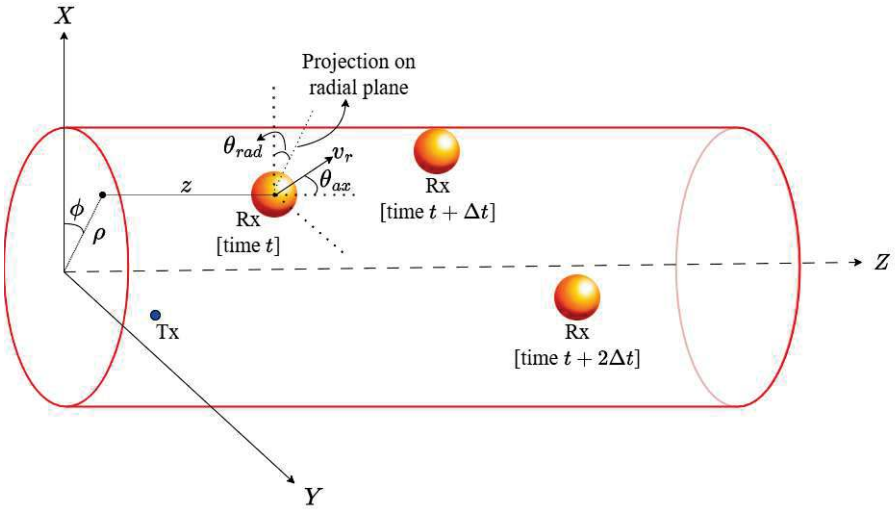

Fig. 2: Mobility of a spherical receiver in a cylindrical channel.

[15], which is used when there is a resistance to mass transfer at the boundary, in equation (10) gives

$$D(t-t_0)\frac{\partial C_{\rho\phi}(t;t_0)}{\partial \rho} = -k_f C_{\rho\phi}(t;t_0) \tag{12}$$

The rate of change of concentration with respect to radial and azimuthal coordinates $C_{\rho\phi}(t;t_0)$ and with respect to axial coordinate $C_z(t;t_0)$ can be given by separating their respective terms from (10) as

$$\begin{aligned}\frac{\partial C_{\rho\phi}(t;t_0)}{\partial t} &= D(t-t_0)\frac{\partial^2 C_{\rho\phi}(t;t_0)}{\partial \rho^2(t)} \\ &+ \frac{D(t-t_0)}{\rho(t)}\frac{\partial C_{\rho\phi}(t;t_0)}{\partial \rho(t)} \\ &+ \frac{D(t-to)}{\rho^2(t)}\frac{\partial^2 C_{\rho\phi}(t;t_0)}{\partial \phi^2(t)} \\ &+ \frac{\delta(\rho(t)-\rho_{tx})}{\rho(t)}\delta(\phi(t)-\phi_{tx})\delta(t-t_0)\end{aligned} \tag{13}$$

$$\begin{aligned}\frac{\partial C_z(t;t_0)}{\partial t} &= D(t-t_0)\frac{\partial^2 C_z(t;t_0)}{\partial z^2(t)} - v\frac{\partial C_z(t;t_0)}{\partial z(t)} \\ &+ \delta(z(t)-z_{tx})\delta(t-t_0) - kC_z(t;t_0)\end{aligned} \tag{14}$$

The solution of (13) is $C_{\rho\phi}(t;t_0)$ given the boundary condition (12),while $C_z(t;t_0)$ is the solution of (14). The detailed solutions of both of these components are explained further.

A. Concentration Green's Function for Axial Component

To solve the CGF (14), the Fourier transform of (14) with respect to z is taken and $D(t)$ is substituted from (5), which leads to

$$\frac{\partial C_\gamma(t;t_0)}{\partial t} = -(D\gamma^2\alpha(t-t_0)^{\alpha-1} + j\gamma v + k)C_\gamma(t;t_0) \tag{15}$$

where $C_\gamma(t;t_0)$ is the Fourier transform of $C_z(t;t_0)$ and the solution for the initial condition of impulsive release is given by

$$C_\gamma(t;t_0) = e^{-((t-t_0)^\alpha D\gamma^2 + j\gamma v(t-t_0) + k(t-t_0))} \tag{16}$$

The CGF for the axial component can be obtained by taking the inverse Fourier transform of (16) as

$$C_z(t;t_0) = \frac{e^{-\frac{(z(t)-z_{tx}-v(t-t_0))^2}{4(t-t_0)^\alpha D} - k(t-t_0)}}{\sqrt{4\pi(t-t_0)^\alpha D}} \tag{17}$$

B. Concentration Green's Function for Radial-Azimuthal Component

Solving the radial-azimuthal equation (13) by the boundary condition (12) and removing the term $\delta(t-t_0)$ (as it is independent from the radial-azimuthal coordinates) from the source term $\frac{\delta(\rho(t)-\rho_{tx})}{\rho(t)}\delta(\phi(t)-\phi_{tx})\delta(t-t_0)$ gives

$$C_{\rho\phi}(t;t_0) = \frac{\delta(\rho(t)-\rho_{tx})}{\rho(t)}\delta(\phi(t)-\phi_{tx}) \tag{18}$$

Now, considering the above condition (12) and removing the source term, the remaining equation in (13) can be solved by means of a variable separation technique [16]. Substituting the value of $C_{\rho\phi}(t;t_0)$ as $C_\rho(t|t_o)C_\phi(t|t_o)C_t(t|t_0)$ in (13) and in the boundary condition (12), dividing both sides of (13) with $C_\rho(\rho(t)|t_o)C_\phi(\phi(t)|t_o)C_t(t|t_0)$, removing the source term, dividing by $\frac{D}{\rho^2(t)}$ and simplifying it will lead to

$$C''_\phi(t;t_0) + \eta C_\phi(t;t_0) = 0 \tag{19}$$

The separation of variables leads to the generation of a constant term η, which accepts the values as $\eta = n^2,\ \forall n \in Z^+$ by considering the concentration to be periodic with period 2π in terms of variable ϕ, $C_\phi(t;t_0) = G_n cos(n(\phi-\phi_{tx}))$. Multiplying it by $\frac{D}{\rho^2(t)}$, which was divided earlier, and by simplifying with simple calculations, yields

$$D\frac{C''_{\rho n}(t;t_0)}{C_{\rho n}(t;t_0)} + \frac{D}{\rho(t)}\frac{C'_{\rho n}(t;t_0)}{C_{\rho n}(t;t_0)} - \frac{Dn^2}{\rho^2(t)} \tag{20}$$

$$= \frac{C'_{tn}(t;t_0)}{\alpha(t-t_o)^{\alpha-1}C_{tn}(t;t_0)} \tag{21}$$

$$= -\psi^2 \tag{22}$$

Here the constant ψ^2 on the right side cannot be non-negative as it will lead to an unbounded concentration function of time. Defining $\lambda_n = \frac{\psi}{\sqrt{D}}$ and considering $D = \rho^2(t)$,

$$\rho^2(t)C''_{\rho n}(t;t_0) + \rho(t)C'_{\rho n}(t;t_0) + C_{\rho n}(t;t_0)(\lambda_n^2\rho^2(t) - n^2) = 0 \tag{23}$$

The solution for the radial component is given by Bessel's equation by considering the boundary condition as

$$C_{\rho_{nm}}(t;t_0) = A_{nm}J_n(\lambda_{nm}\rho(t)) \tag{24}$$

where, A_{nm} is a constant, λ_{nm} is the eigenvalue and $J_n(.)$ is the n^{th} order Bessel function of the first kind. Considering the time component $\frac{C'_{tn}(t;t_0)}{\alpha(t-t_o)^{\alpha-1}C_{tn}(t;t_0)}$ in (20), the solution of the above equation is obtained by considering the condition of $\lim_{t\to\infty} C_t(t;t_0) = 0$ as

$$C_{t_{nm}}(t;t_0) = I_{nm}e^{-D\lambda_{nm}^2(t-t_o)^\alpha} \tag{25}$$

Therefore combining all the components, i.e. the radial, azimuthal, and time, gives

$$\begin{aligned}C_{\rho\phi}(t;t_0) = \sum_{n=0}^{\infty}\sum_{m=1}^{\infty} & G_n cos(n(\phi(t)-\phi_{tx})) \\ & \times A_{nm}J_n(\lambda_{nm}\rho(t)) \\ & \times I_{nm}e^{-D\lambda_{nm}^2(t-t_o)^\alpha}u(t-t_o)\end{aligned} \tag{26}$$

with $A_{nm}I_{nm}G_{nm} = \frac{L_n J_n(\lambda_{nm}\rho_{tx})}{N_{nm}}$, such that

$$\begin{aligned}C(t;t_0) = \frac{e^{-\frac{(z(t)-z_{tx}-v(t-t_0))^2}{4(t-t_0)^\alpha D} - k(t-t_0)}}{\sqrt{4\pi(t-t_0)^\alpha D}} & \sum_{n=0}^{\infty}\sum_{m=1}^{\infty} G_n\cos(n(\phi(t)-\phi_{tx})) \times A_{nm}J_n(\lambda_{nm}\rho(t)) \\ & \times I_{nm}e^{-D\lambda_{nm}^2(t-t_0)^\alpha}u(t-t_0)\end{aligned} \tag{27}$$

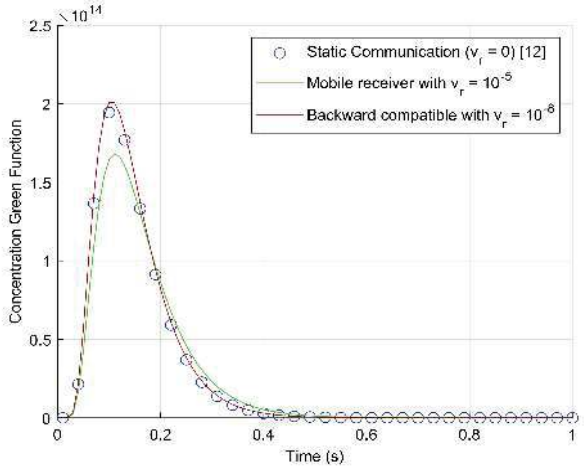

Fig. 4: Backward compatibility with static communication.

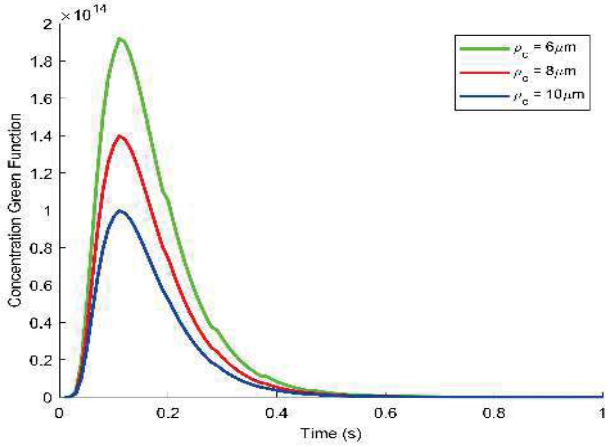

Fig. 5: CGF obtained analytically by considering different values of channel radius $\rho_c = 6\mu m,\ 8\mu m,\ 10\mu m$.

$$L_n = \begin{cases} \frac{1}{\pi}, & \text{if } n \geq 1 \\ \frac{1}{2\pi}, & \text{if } n = 0 \end{cases}$$

$N_{nm} = \frac{\rho_c^2}{2}(J_n^2(\lambda_{nm}\rho_c) - J_{n-1}(\lambda_{nm}\rho_c)J_{n+1}(\lambda_{nm}\rho_c))$ and ρ_c is the channel radius. Hence, combining the axial and radial-azimuthal components, the final CGF expression is obtained as shown in (27).

C. Interference Limit at the Primary Receiver

As per our network model, there exist multiple links communicating simultaneously with each other. In this work, the priority of the primary link is considered higher as compared to that of the secondary link, and hence the interference at the primary receiver should be minimal. This could be fulfilled by limiting the number of molecules transmitted by the secondary transmitter. Also, the interference could be from the molecules transmitted in the previous time slots, referred to as Inter Symbol Interference (ISI), which also needs to be taken into account. In this section, an expression is derived for the number of molecules that can be transmitted by the secondary transmitter in order to minimize the interference at the primary receiver following an underlay-cognitive communication method.

The average number of molecules that can be transmitted by a secondary transmitter taking the ISI into account is given as [17]

$$\mathbb{E}[N(RX_p; TX_s)] \leq \lambda_U \tag{28}$$

where, $N(RX_p; TX_s)$ is the number of molecules that are transmitted by the secondary transmitter and received by the primary receiver and λ_U is the maximum limit for interference. $\mathbb{E}[N(RX_p; TX_s)]$ can be solved further as,

$$\mathbb{E}[N(RX_p; TX_s)] = \sum_{k=1}^{t} (\mathbb{E}[N(t;k)|b(s;k) = 1] \times p(b(s;k) = 1) + \mathbb{E}[N(t;k)|b(s;k) = 0] \times p(b(s;k) = 0)) \tag{29}$$

In (29), $[N(t;k)|b(s;k)]$ is the number of molecules transmitted in the k_{th} slot and received in the t_{th} slot when the bit b is transmitted and $p(b(s;k))$ is the probability of the bit b to occur. The mean number of molecules during the transmission of bit "0" is 0. Hence,

$$\sum_{k=1}^{t} \Big(N(t;\hat{d}) \Big| TX_s \Big) \times p\Big((t;k) \Big| (RX_p; TX_s) \Big) \leq \lambda_U \tag{30}$$

The term $\hat{d}$ is the distance between the secondary transmitter and the primary receiver. Here, the maximum number of molecules that can be transmitted by a transmitter in the current time slot is given as,

$$\begin{aligned} N\Big(0;\hat{d}\Big|TX_s\Big) \leq \frac{1}{p\Big(t;t\Big|(RX_p;TX_s)\Big)} \times \Bigg[& \frac{\lambda_u}{P(b(s;k)=1)} \\ & - \sum_{k=1}^{t-1} N\Big(t-k;\hat{d}\Big|TX_s\Big) \\ & \times p\Big((t;k)\Big|(RX_p;TX_s)\Big)\Bigg] \\ = s & \end{aligned} \tag{31}$$

Now, in order to maintain certain Quality of Standards (QOS), the secondary transmitter cannot transmit molecules greater than λ_L. Hence, the total number of molecules that the secondary transmitter can transmit is,

$$N\Big(0;\hat{d}\Big|TX_s\Big) = min\Big[\lambda_L, max(0,s)\Big] \tag{32}$$

Note that in Figs. 4, 5, 6, the CGF for the position vector corresponding to the primary receiver are plotted. Nonetheless, the system model of the secondary receiver would be akin to the system model of the primary receiver, with the only difference being the secondary transmitter will now be the primary transmitter and vice versa in the formulation of the system model.

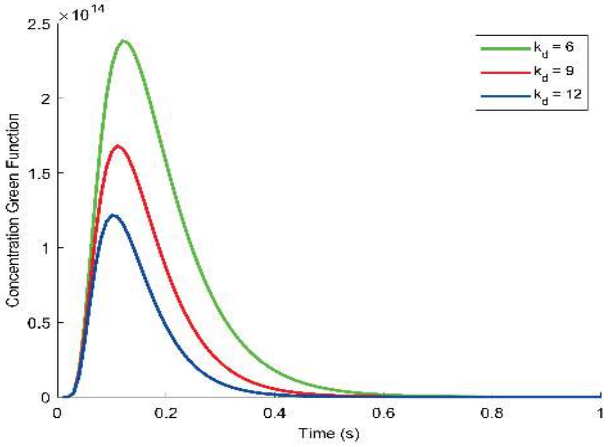

Fig. 6: CGF obatined analytically by considering different values of degradation constant, $k_d = 6,\ 9,\ 12$.

TABLE I: Summary of the notations used in this work.

Notation	Description	Value
D	Diffusion Coefficient	$10^{-10}\,\mathrm{m^2 s^{-1}}$
k	Degradation rate	$9\,\mathrm{s^{-1}}$
v	Drift velocity	$60\,\mu\mathrm{m\,s^{-1}}$
ρ_c	Channel Radius	$5\,\mu$m
R	Receiver Radius	$2\,\mu$m
$(\rho_{TX_p}, \phi_{TX_p}, z_{TX_p})$	Primary Transmitter Position	$(2\,\mu\mathrm{m}, \pi, 0)$
$(\rho_{RX_p}, \phi_{RX_p}, z_{RX_p})$	Primary Receiver Position	$(2\,\mu\mathrm{m}, 0, 10\,\mu\mathrm{m})$
$(\rho_{TX_s}, \phi_{TX_s}, z_{TX_s})$	Secondary Transmitter Position	$(2\,\mu\mathrm{m}, 0, 0)$
$(\rho_{RX_s}, \phi_{RX_s}, z_{RX_s})$	Secondary Receiver Position	$(3\,\mu\mathrm{m}, \pi, 10\,\mu\mathrm{m})$
N_{TX_p}	Molecules Transmitted by TX_p	3000

IV. NUMERICAL RESULTS

The CGF that is derived above considering mobile receiver is depicted in Fig. 4. where it is evident that while considering the mobile receiver in a DMC channel with $v = 10^{-5}\ m/s$, lower CGF is observed at the receiving end which is correct as the receiver is moving in the channel and hence the concentration should be less as compared to the static receiver. Fig. 4 proves the backward compatibility with the static communication [12] by taking the sufficiently low value of receiver velocity(v_r), roughly equal to $10^{-8}\ m/s$ which means that the receiver is almost static. Since the CGF of the static receiver matches that of the receiver with a velocity close to zero, it can be concluded that the analytical derivations are correct, as they are backward compatible with static communication.

Additionally, the effect of considering different system parameters on the CGF is analyzed. Fig. 5 shows the change in the CGF with varying channel radius (ρ_c) by using the values from Table I. It can be observed that as the channel radius decreases from $10\ \mu m$ to $6\ \mu m$, the number of molecules absorbed at the receiver increases. This implies that narrowing the channel, improves the signal strength and in turn increases the channel performance. Fig. 6 shows the effect of the degradation constant on the channel performance by considering $k_d = 6,\ 9$ and 12. On increasing the degradation constant, CGF decreases as a larger number of molecules is degraded with an increase in k_d, which leads to less number of molecules available to make the bond with the receiver. Hence it is evident that our analytical derivations align with the real-world scenario, aiding efforts for realistic channel modeling for targeted drug delivery.

V. CONCLUSION

In this work, a realistic molecular communication scenario is analyzed considering mobile molecular communication in a cylindrical blood vessel like channel with the existence of multiple links within, with the aim of furthering progress toward targeted drug delivery. A CGF is derived for the axial and radial-azimuthal components, and the analysis is validated by proving its backward compatibility with the static MC system.

REFERENCES

[1] M. Ş. Kuran, H. B. Yilmaz, T. Tugcu, and B. Özerman, "Energy model for communication via diffusion in nanonetworks," *Nano Commun. Networks*, vol. 1, no. 2, pp. 86–95, 2010.

[2] M. Pierobon and I. F. Akyildiz, "Diffusion-based noise analysis for molecular communication in nanonetworks," *IEEE Trans. Signal Process.*, vol. 59, no. 6, pp. 2532–2547, 2011.

[3] M. M. Al-Zu'bi and A. S. Mohan, "Modeling of ligand-receptor protein interaction in biodegradable spherical bounded biological micro-environments," *IEEE Access*, vol. 6, pp. 25 007–25 018, 2018.

[4] N. Farsad, A. W. Eckford, S. Hiyama, and Y. Moritani, "On-chip molecular communication: Analysis and design," *IEEE Trans. Nanobiosci.*, vol. 11, no. 3, pp. 304–314, 2012.

[5] M. Zoofaghari and H. Arjmandi, "Diffusive molecular communication in biological cylindrical environment," *IEEE Trans. Nanobiosci.*, vol. 18, no. 1, pp. 74–83, 2018.

[6] A. W. Eckford, "Achievable information rates for molecular communication with distinct molecules," in *2007 2nd Bio-Inspired Models of Network, Information and Computing Systems*. IEEE, 2007, pp. 313–315.

[7] L. Felicetti, M. Femminella, and G. Reali, "Establishing digital molecular communications in blood vessels," in *2013 First International Black Sea Conference on Communications and Networking (BlackSeaCom)*. IEEE, 2013, pp. 54–58.

[8] A. Guney, B. Atakan, and O. B. Akan, "Mobile ad hoc nanonetworks with collision-based molecular communication," *IEEE Trans. Mob. Comput.*, vol. 11, no. 3, pp. 353–366, 2011.

[9] Y. Okaie and T. Nakano, "Mobile molecular communication through multiple measurements of the concentration of molecules," *IEEE Access*, vol. 8, pp. 179 606–179 615, 2020.

[10] R. Mosayebi, A. Ahmadzadeh, W. Wicke, V. Jamali, R. Schober, and M. Nasiri-Kenari, "Early cancer detection in blood vessels using mobile nanosensors," *IEEE Trans. Nanobiosci.*, vol. 18, no. 2, pp. 103–116, 2018.

[11] A. Goldsmith, S. A. Jafar, I. Maric, and S. Srinivasa, "Breaking spectrum gridlock with cognitive radios: An information theoretic perspective," *Proc. IEEE*, vol. 97, no. 5, pp. 894–914, 2009.

[12] S. Dhok, P. Peshwe, and P. K. Sharma, "Cognitive molecular communication in cylindrical anomalous-diffusive channel," *IEEE Trans. Mol. Biol. Multi-Scale Commun.*, 2021.

[13] J. Philibert, "One and a half century of diffusion: Fick, einstein," *Diffusion Fundamentals: Leipzig 2005*, vol. 1, p. 8, 2005.

[14] J.-H. Jeon, A. V. Chechkin, and R. Metzler, "Scaled brownian motion: a paradoxical process with a time dependent diffusivity for the description of anomalous diffusion," *Phys. Chem. Chem. Phys.*, vol. 16, no. 30, pp. 15 811–15 817, 2014.

[15] Y. Deng, A. Noel, M. Elkashlan, A. Nallanathan, and K. C. Cheung, "Modeling and simulation of molecular communication systems with a reversible adsorption receiver," *IEEE Trans. Mol. Biol. Multi-Scale Commun.*, vol. 1, no. 4, pp. 347–362, 2015.

[16] K. Cole, J. Beck, A. Haji-Sheikh, and B. Litkouhi, *Heat conduction using Greens functions*. CRC Press, 2010.

[17] N. V. Sabu, N. Varshney, and A. K. Gupta, "On the performance of the primary and secondary links in a 3-d underlay cognitive molecular communication," *IEEE Transactions on Communications*, vol. 69, no. 12, pp. 8028–8041, 2021.